

Star-Shaped Molecules with Polyhedral Oligomeric Silsesquioxane Core and Azobenzene Dye Arms

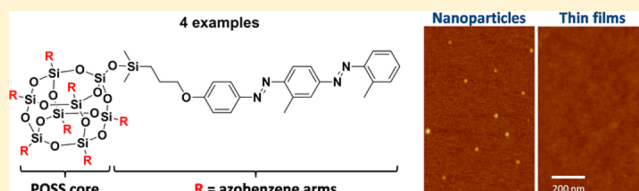
Petr A. Ledin,[†] Ihor M. Tkachenko,[‡] Weinan Xu,[†] Ikjun Choi,[†] Valery V. Shevchenko,[‡] and Vladimir V. Tsukruk^{*,†}

[†]School of Materials Science and Engineering, Georgia Institute of Technology, Atlanta, Georgia 30332, United States

[‡]Institute of Macromolecular Chemistry, National Academy of Sciences of Ukraine, Kharkovskoe shosse 48, Kiev, 02160, Ukraine

Supporting Information

ABSTRACT: We synthesized a series of hybrid nanomaterials combining organic dyes with polyhedral oligomeric silsesquioxanes (POSS) based on three different azobenzenes: monoazobenzene (4-phenylazophenol), bis-azobenzene (Disperse Yellow 7 and Fast Garnet derivative), and push–pull azobenzene (Disperse Red 1) via hydrosilylation coupling. The azo-functionalized POSS compounds possess high thermal stability, and their branched architecture resulted in effective suppression of molecular aggregation and allowed for direct imaging of individual dye–POSS structures with expected molecular dimensions. Stable, uniform, smooth, and ultrathin nanocomposite films with mixed silica–organic composition and relatively low refractive indices can be fabricated from all azo–POSS branched conjugates. Finally, the photoisomerization behavior of POSS-conjugated 4-phenylazophenol was investigated in solution as well as in ultrathin nanocomposite film. We found that conjugation to POSS core did not affect the kinetics of trans–cis photoisomerization and thermal cis–trans relaxation. Furthermore, rapid and reversible photoisomerization was observed in azo–POSS nanocomposite films. We suggest that the highly stable branched azo–POSS conjugates with high dye grafting density described here can be considered for nanometer-sized photoswitches, active layer material with optical-limiting properties, and a medium with photoinduced anisotropy for optical storage.



INTRODUCTION

Organic–inorganic oligomeric silsesquioxanes with a general formula $\text{RSiO}_{3/2}$ are widely used to improve the thermal, mechanical, and optical properties of nanocomposite materials.^{1–3} Well-defined cubic cage structures, termed polyhedral oligosilsesquioxanes (POSS), are particularly attractive as building blocks and scaffolds due to their monodispersity, ease of preparation, and covalent functionalization.^{4–7} Conjugation of small organic molecules to a POSS core results in novel hybrid materials with unique physical characteristics.^{8,9} For example, attachment of hydrogen-bonding groups to oligomeric silsesquioxanes enables formation of supramolecular polymers.¹⁰ POSS modification with ionic groups opens the possibility to prepare thin films using a layer-by-layer (LbL) assembly technique.¹¹ Furthermore, complexation with metals is possible when the POSS cage is modified with chelating moieties.^{12,13} Conjugation of organic chromophores to POSS core was shown to increase the thermo- and photostability of dyes and enhance optical properties.¹⁴ Furthermore, the bulky POSS core disrupts the stacking of conjugated molecules, therefore increasing fluorescence efficiency.^{15,16} The amorphous character of these conjugates results in solution processability, which makes it possible to manufacture nanocomposites by versatile wet chemistry approaches.^{17,18}

Organic dyes containing an azobenzene fragment are used extensively as tunable chromophores and light-responsive

moieties due to reversible trans–cis photoisomerization.^{19,20} Photoresponsive azobenzene behavior has been the subject of an intensive research, which resulted in a good understanding of the properties of azobenzene-containing molecules in solution as well as thin films and molecular monolayers.^{21,22} So far, in order to obtain processable materials, azo groups were introduced into main and side chains of various polymers.^{23,24} These materials were shown to exhibit photoinduced birefringence,²⁵ dichroism,²⁶ and photoactuation properties.^{27,28} Applications in optics and photonics require the active material to have high photo- and thermostability and optical transparency.^{29,30} Therefore, attachment of photoresponsive azo dyes to POSS may result in novel hybrid materials with broad applications. Several recent studies demonstrated the utility of this approach by grafting simple azobenzenes onto cubic POSS cages.

In fact, Chi et al. showed that monofunctionalization of POSS by a single dye increased the decomposition temperature of a resulting conjugate by 177 °C comparing to the initial dye.³¹ POSS cages functionalized with one, two, and three azobenzene moieties at a single corner by Zhou et al. also showed high thermal stability and rapid photoisomerization in

Received: May 19, 2014

Revised: July 9, 2014

Published: July 10, 2014

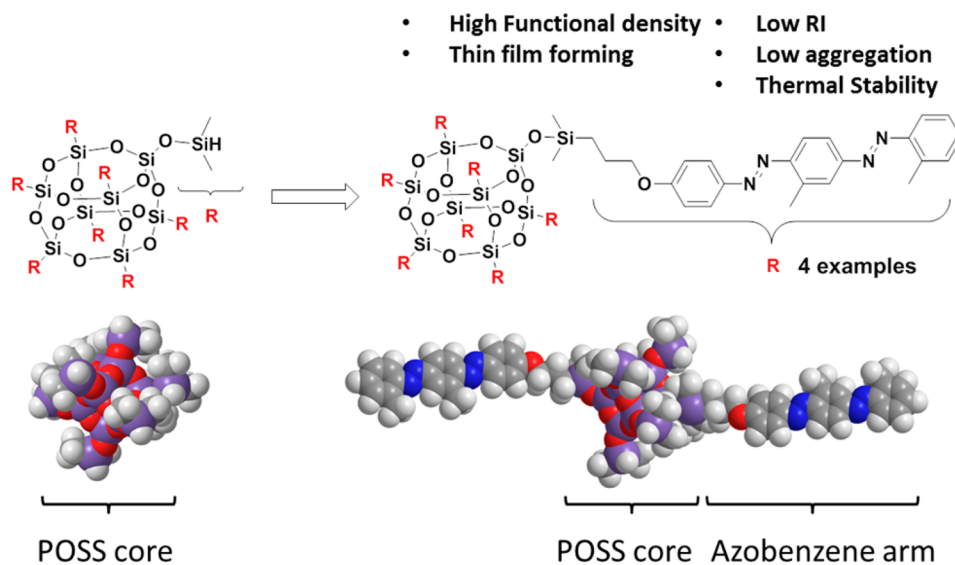
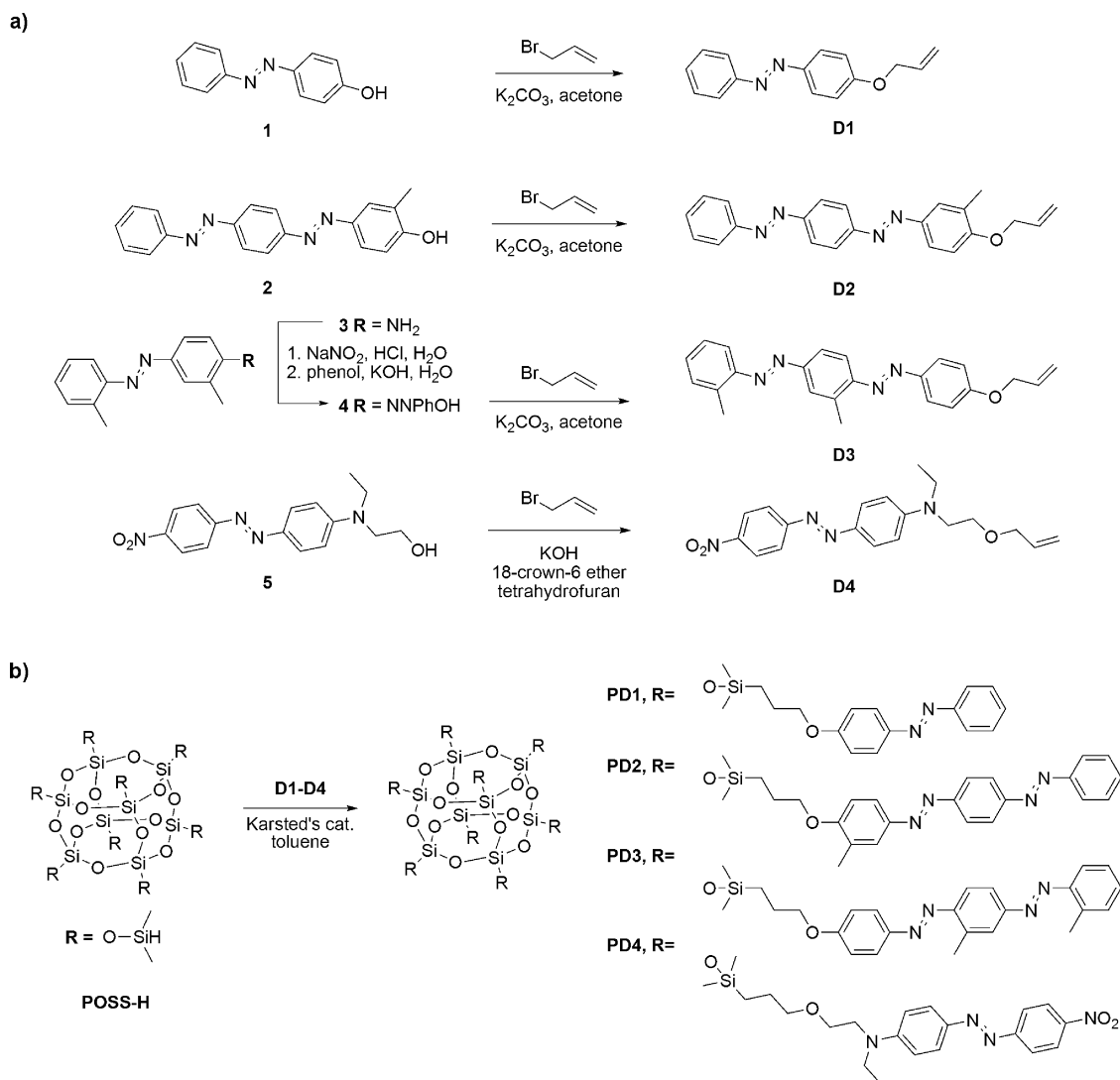


Figure 1. Preparation of azo-POSS conjugates implemented in this study. Only two azobenzene arms are depicted for clarity.

Scheme 1. Synthetic path for compounds D1–D4 (a) and PD1–PD4 (b)



solution.³² Finally, Miniewicz et al. demonstrated the photo-induced birefringence variation by mixing azo-functionalized

POSS into a liquid crystalline matrix.³³ Substitution of an azobenzene fragment strongly affects the azobenzene absorb-

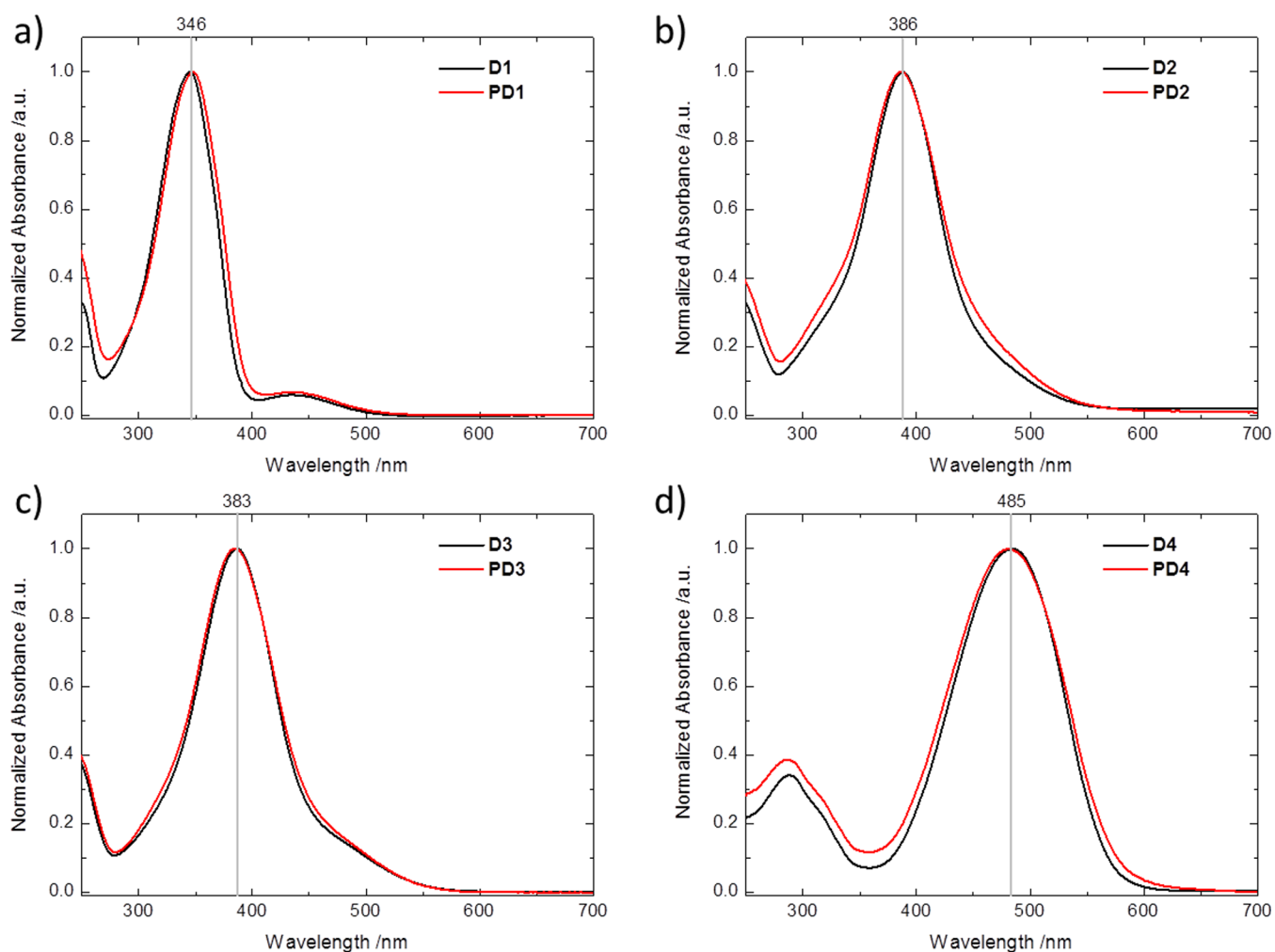


Figure 2. (a–d) UV–vis absorbance spectra of D1–D4 and respective conjugates PD1–PD4 in CHCl_3 (0.01 mg/mL).

ance spectra and isomerization behavior. Simple azobenzene derivatives such as those prepared from 4-phenylazophenol (Solvent Yellow 7) with well-separated π – π^* and n – π^* transitions have been demonstrated to have a relatively low rate of *cis*–*trans* isomerization, which can take days in the dark. On the other hand, push–pull azobenzene derivatives, such as *N*-ethyl-*N*-(2-hydroxyethyl)-4-(4-nitrophenylazo)aniline (Disperse Red 1) have a red-shifted π – π^* azobenzene absorbance and a very low energy barrier between two isomers. By increasing the number of photochromic groups in bis-azobenzenes, such as Disperse Yellow 7, it is possible to achieve higher photoinduced anisotropy than in monoazobenzene-based materials.³⁴ To the best of our knowledge, multiarm conjugation of bis-azo and push–pull azo dyes to POSS cores has not been reported yet. Despite the large variety of synthetic methods available for POSS modification, steric hindrance and hydrolytic instability under the basic conditions of octameric silsesquioxanes may complicate the synthesis of monodisperse conjugates with large number of arms.³⁵

Thus, here we focus on the synthesis of novel dye-modified POSS cages that can be achieved either by hydrolysis–condensation of appropriately substituted alkoxy silanes or by using functionalized POSS cages for covalent attachment of a series of organic dye molecules with large (>80%) substitution (Figure 1).^{36,37}

In this work, we prepared a series of highly substituted azo–POSS structures based on three different classes of azobenzenes: monoazobenzene (4-phenylazophenol), bis-azobenzene (Disperse Yellow 7), and push–pull azobenzene [Disperse Red 1 (DR-1)] via hydrosilylation coupling (Scheme 1). For these compounds, a degree of functionalization within 80–90% was achieved according to nuclear magnetic resonance (NMR) spectroscopy data. We found that thermal stability strongly depends on the type of organic substituent, with simple monoazobenzene having the highest decomposition temperature and the DR-1 derivative the lowest. All conjugates were shown to have a glass transitions in a range from 10 to 70 °C. Due to the amorphous character of conjugates, stable uniform ultrathin films could be prepared by spin-coating from organic solutions of azo–POSS conjugates. Finally, photoisomerization behavior of POSS-conjugated 4-phenylazophenol was investigated in solution as well as in thin film, and preservation of photophysical properties was observed in conjugated azo–POSS materials.

RESULTS AND DISCUSSION

Synthesis and Characterization of Azo–POSS Conjugates. Hydrosilylation is a reliable method for Si–C bond formation under Pt(0) catalysis. We chose an octakis-(dimethylsilyloxy)silsesquioxane (POSS-H) as a scaffold for attachment of a variety of azo dyes bearing reactive allyloxy

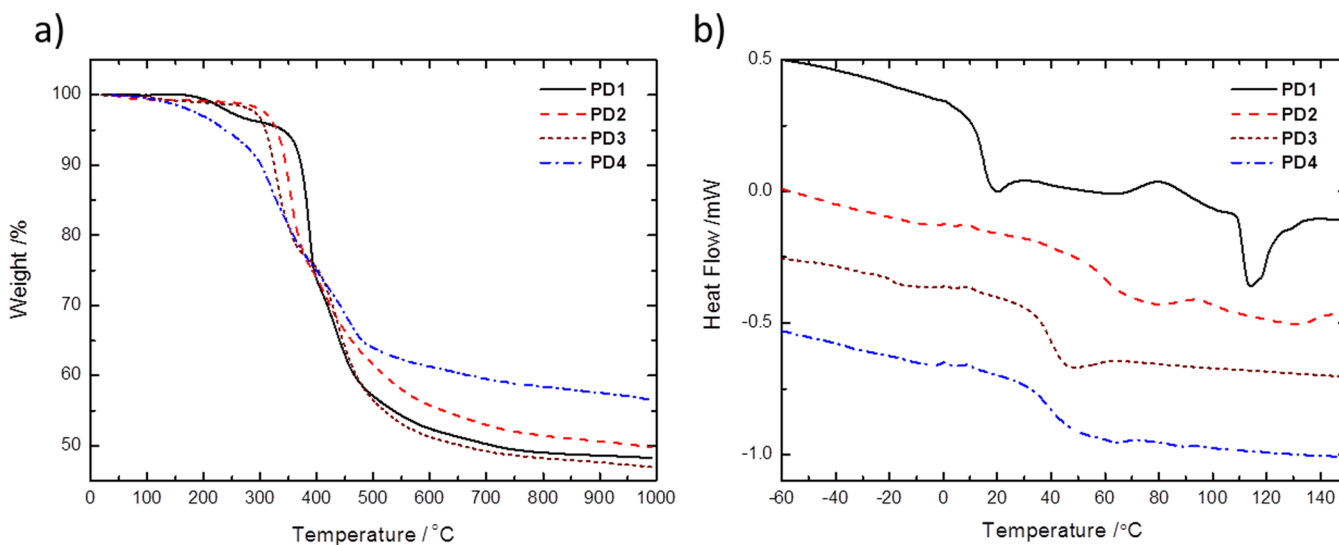


Figure 3. TGA (a) and DSC (b) curves of POSS–dye conjugates **PD1–PD4**. DSC curves are offset for clarity.

groups. Commercially available azo dyes served as precursors for synthesis of compounds **D1–D4** (Scheme 1a). The allyl handle for the subsequent hydrosilylation reaction was introduced by etherification of the corresponding alcohols with allyl bromide in the presence of potassium carbonate, or potassium hydroxide as a base. **D1**, **D2**, and **D4** were prepared from 4-phenylazophenol (**1**), Disperse Yellow 7 (**2**), and Disperse Red 1 (**5**), respectively, with yields of 62–82%. Similarly, **D3** was prepared from compound (**4**) obtained by diazotation of Fast Garnet (**3**) followed by phenol coupling. Compounds **D1–D4** were obtained as pure crystalline orange-brown-colored solids. (See the Supporting Information for NMR and Fourier transform infrared spectroscopy (FTIR) spectra).

Having a series of functionalized dyes with absorption covering a spectral range from 350 (**D1**) to 480 nm (**D4**) in hand, we moved to preparation of substituted POSS–Dye (**PD**) conjugates (Scheme 1b). In a typical procedure, hydrosilylation was conducted by stirring octakis-(dimethylsilyloxy)silsesquioxane with 8 equiv of respective allyloxy derivative (**D1–D4**) in dry toluene at 40 °C in the presence of 2 mol % of platinum(0)-1,3-divinyl-1,1,3,3-tetramethyldisiloxane.

It has to be noted that the increase of the hydrosilylation reaction temperature to 100 °C facilitates the carbon–carbon double bond reduction of the dyes. The formation of hydrogenation side products is known to occur in hydrosilylation reactions.³⁸ The reactions were terminated after 72 h and the products were isolated by evaporation of solvent followed by silica-gel chromatography. The purification gave compounds **PD1–PD4** in yields of 22–53%. The successful grafting of dyes onto POSS–H was indicated by IR spectra, which showed the disappearance of the Si–H stretching band at 2140 cm^{-1} (Supporting Information). Furthermore, both sets of signals from the POSS core (Si–C at 1250 cm^{-1} , Si–O–Si at 1090 cm^{-1}) and aromatic dyes (C–H at 3050 cm^{-1} , C=C at 1600 and 1500 cm^{-1}) were present in the conjugate's spectra. ^1H NMR spectroscopy indicated nearly complete modification of the octavalent POSS core with azo dyes. From comparison of the integral areas of CH_3 proton signals of the POSS cage and the total integral area of attached dye molecules, the degree of functionalization can be obtained

(Supporting Information). According to these calculations, the degree of functionalization was 90% for **PD1**, 80% for **PD2**, 88% for **PD3**, and 81% for **PD4**. It is noteworthy that the increase of the reaction time from 72 to 150 h did not result in a higher degree of POSS functionalization.

Compound **D1** has a typical azobenzene absorbance with a strong π – π^* band at 348 nm and a weaker n – π^* transition at around 430 nm (Figure 2a). The substitution of an electron-donating NH_2 group of Fast Garnet (compound **3**) with an allyloxyphenyldiazene fragments leads to the hypsochromic shift of **D3** absorbance in the UV–vis spectrum comparing to a parent compound. Therefore, a pair of bis-azobenzene dyes, **D2** and **D3**, have almost identical absorbance spectra with an absorbance maxima, corresponding to the π – π^* transition, at around 385 nm (Figure 2b,c). In this case, the n – π^* transition appears as a shoulder of a main peak at around 470 nm.

Dye **D4** derived from Disperse Red 1 (**5**) has the characteristic absorbance spectra of push–pull azobenzene molecules, with overlapping π – π^* and n – π^* transitions, resulting in a single absorbance peak at around 485 nm (Figure 2d). The π – π^* transition of azo dyes is sensitive to aggregation. In particular, a hypsochromic shift is observed when azobenzene molecules form H-aggregates.³⁹ The absence of a pronounced shift of absorbance peak positions before and after dye conjugation to the POSS core indicates that in dilute solution aggregation is insignificant. Moreover, the proximity of the azobenzene molecules attached to the cubic POSS core also does not induce intramolecular stacking. Azo dyes are poor fluorescence emitters, as the nonradiative decay of the photoexcited state through isomerization dominates the radiative pathway with quantum yields of around 10^{-3} reported for DR-1.⁴⁰ We observed only a very weak fluorescence around 580 nm ($\lambda_{\text{ex}} = 490$ nm) with a Stokes shift of 90 nm in chloroform solutions of **D4** and **PD4**⁴¹ (Supporting Information).

Thermal Properties of Azo–POSS Conjugates. In order to evaluate the thermal stability of POSS–dye conjugates, thermogravimetric analysis (TGA) was performed in an atmosphere of nitrogen (Figure 3a; see the Supporting Information for a derivative plot). In general, TGA of compounds featured two decomposition steps. Apparently, the first decomposition corresponds to the cleavage of the azo

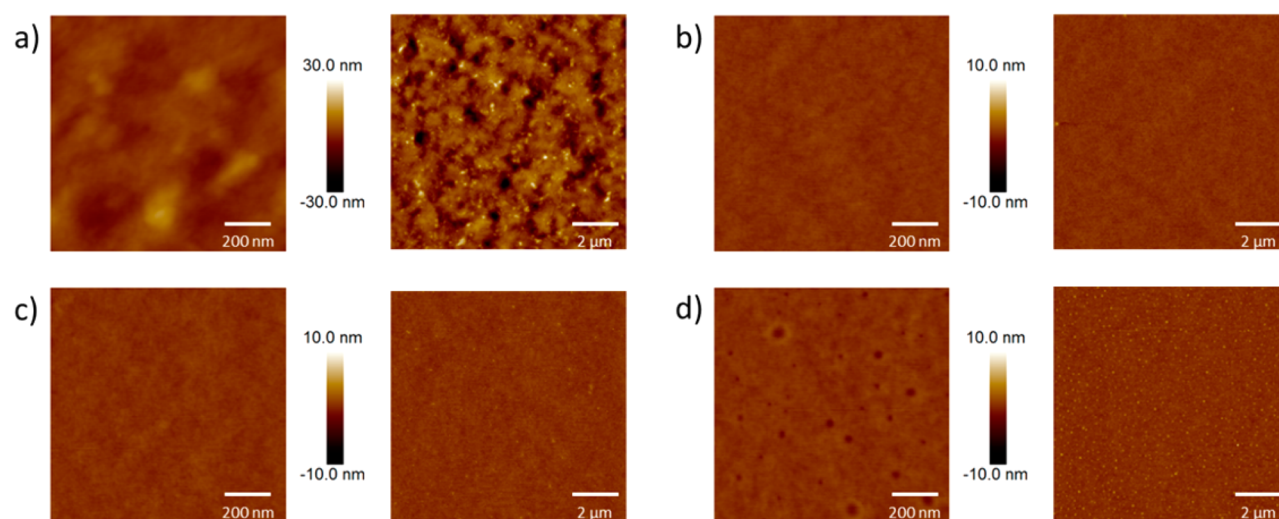


Figure 4. (Left) $1 \times 1 \mu\text{m}^2$ and (right) $10 \times 10 \mu\text{m}^2$ AFM images of thin films prepared by spin-coating from 20 mg/mL solution in toluene at 3000 rpm: (a) PD1, (b) PD2, and (c) PD3. (d) Images of PD4 spin-coated from 10 mg/mL solution in toluene at 3000 rpm. The z-scale is 60 nm for PD1 and 20 nm for PD2–PD4.

Table 1. Optical Characteristics of Ultrathin Films of Azo–POSS Conjugates

compd	$\lambda_{\text{max}}^a, \lambda_{\text{max}}^b$ (nm)	k^b	α (10^5 cm^{-1})	$n(\lambda_{\text{max}})$	n_{max} (at λ , nm)	d (nm) ^b
PD1	346, 340	0.32	1.16	1.62	1.81 (385)	60.1
PD2	386, 384	0.41	1.33	1.60	1.81 (435)	56.0
PD3	383, 384	0.48	1.57	1.59	1.86 (437)	57.9
PD4	480, 484	0.35	0.92	1.59	1.81 (560)	7.9 ^c (124.6) ^d

^aDetermined by UV–vis spectroscopy of a thin film. ^bOn the basis of spectroscopic ellipsometry. ^cFor the film obtained by spin-coating from 10 mg/mL solution in toluene at 3000 rpm. ^dFor the film obtained by spin-coating from 20 mg/mL solution in chloroform at 500 rpm.

group between 250 and 400 °C.⁴² The second stage between 400 and 500 °C corresponds to decomposition of the remaining organic fragments and the POSS core. The decomposition temperatures were then determined as a temperature at which the weight loss reaches 5%. PD1 has the highest thermal stability with a decomposition temperature of 340 °C and a peak weight loss rate at around 390 °C. Compounds PD2 and PD3 had identical onset of decomposition, with decomposition temperatures of 320 and 310 °C, respectively. Compound PD4 was the least stable out of the four azo–POSS derivatives, with a decomposition temperature of 240 °C.

Decomposition of substituted oligomeric silsesquioxane depends strongly on the nature of the grafted organic groups. In general, POSS derivatives with small aliphatic side chains sublime during TGA in the absence of oxygen and have relatively low char yield.⁴³ Larger aliphatic and aromatic substituents prevent sublimation, and polymerization of the POSS cage may occur, which hinders the release of the gaseous products of decomposition, resulting in a larger amount of residue.^{44,45} Indeed, for azo–POSS conjugates PD1–PD4 we observed a char yield of 50–60% after heating to 1000 °C. The relatively low decomposition temperature of PD4 can be explained by an early loss of a nitro group and the larger saturated aliphatic portion of D4 comparing to the other dyes in this study.

Thermal properties of PD1–PD4 were further investigated using differential scanning calorimetry (DSC) (Figure 3b). The DSC was performed in a temperature range of –80 to 200 °C with heating and cooling rates of 10 °C/min. The second heating cycle was used to determine the glass transition

temperatures of the conjugates. As determined from the inflection point position on the DSC curve, PD1 has a T_g of 14 °C. A small crystallization peak was observed at 80 °C, followed by melting at 114 °C. In contrast, compounds PD2–PD4 only showed glass transitions at 60, 38, and 40 °C, respectively, without apparent melting transitions. The effect of POSS cores on inhibiting the crystallization process is well-documented.⁴⁶ The bulky POSS cage and short spacers disrupt the packing of its azobenzene arms into a crystal lattice.

Thin films Prepared from Azo–POSS Conjugates. We contemplated that the amorphous character of azo–POSS conjugates will facilitate the formation of uniform ultrathin films as opposed to unmodified dyes. We therefore investigated the formation of thin films from azo–POSS conjugates PD1–PD3 by spin-coating toluene solution (20 mg/mL) onto quartz and silicon substrates. PD4 has a lower solubility in toluene and therefore 10 mg/mL solution was used for spin-coating. Atomic force microscopy (AFM) imaging revealed diverse but uniform surface morphologies of thin films derived from azo–POSS conjugates based on different azo dyes (Figure 4).

The thickness of the resulting films was estimated using spectroscopic ellipsometry to be 60.1, 56.0, 57.9, and 7.9 nm for PD1, PD2, PD3, and PD4 respectively (Table 1). Ultrathin films prepared from PD2 and PD3 had an extremely smooth surface with root-mean-square (RMS) roughness of 0.32 and 0.31 nm, respectively, as determined based on $1 \times 1 \mu\text{m}^2$ AFM scans (here and hereafter). PD1, on the other hand, under the same conditions formed a relatively rough film, with a roughness of 3.2 nm. In this case, formation of crystalline domains and up to 30 nm deep cavities was observed on the film surface. The thin film prepared from PD4 had a smooth

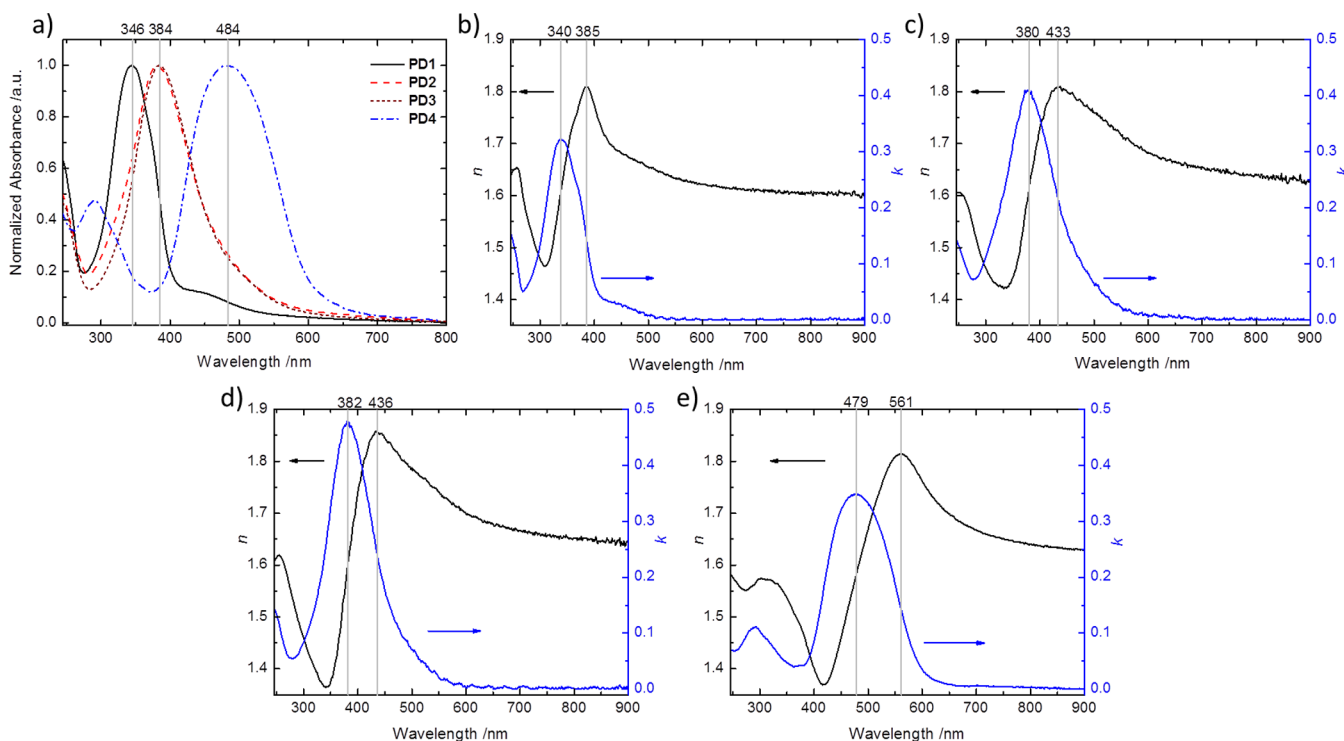


Figure 5. (a) UV-vis absorbance spectra of PD1–PD4 thin films on quartz substrate. Dispersion curves for compounds PD1–PD4 determined from spectroscopic ellipsometry, where n and k are the real and imaginary parts of the complex refractive index, respectively: (b) PD1, (c) PD2, (d) PD3, and (e) PD4.

surface with microroughness of 0.36 nm. We observed small 2–3 nm deep circular cavities on the film surface. The possibility of film dewetting was ruled out by annealing the sample for 3 h at 80 °C, after which the cavities became less pronounced (Supporting Information). These cavities could originate from the residual moisture absorbed by the relatively polar PD4 compound. In general, it appears that the larger organic component of bis-azobenzenes D2 and D3 has a positive effect on the film-forming properties of azo-based POSS conjugates. Attempts to produce continuous films from dyes D1–D4 were unsuccessful due to crystallization of organic compounds. The UV-vis absorption spectra of POSS–dye conjugates spin-coated on quartz slides closely resembled solution spectra (Figure 5a). The peak positions were identical for PD2 and PD3 at 384 nm, 346 nm for PD1, and 484 nm for PD4 (Figure 5a).

POSS doping is used extensively to improve the optical properties of materials, due to the low refractive index and scattering of oligomeric silsesquioxanes.⁴⁷ Thus, for testing optical properties, we determined the real (n) and imaginary parts (k) of a complex refractive index of PD conjugates over a spectral range from 245 to 900 nm by using spectroscopic ellipsometry (SE) (Figure 5b–e). Since the spin-coated film from PD4 was too thin for reliable measurement of optical constants, we conducted these measurements on a 125-nm-thick film obtained by spin-coating of PD4 from a solution in CHCl₃ (20 mg/mL) at 500 rpm.

The extinction coefficients (k) obtained for PD1–PD4 from SE match closely with UV-vis absorbance spectra in Figure 5a. Peak positions are tabulated in Table 1 along with corresponding data from UV-vis absorbance spectra. The molar extinction coefficient (α) can be estimated from k using the following equation: $\alpha = 4\pi k_{\max}/\lambda_{\max}$. The real refractive

index (n) values for conjugates PD1–PD4 fall within a range of 1.59 to 1.62 at the absorption maxima (λ_{\max}). The maximum value of n for PD1, PD2, and PD4 is 1.81 at 385, 435, and 560 nm, respectively. Compound PD3 had a highest real refractive index of 1.86 at 437 nm according to SE. These parameters are comparable with traditional low refractive index materials based on azobenzenes and polycarbonates or polyacrylates.⁴⁸

Individual Azo-POSS Conjugates. Unique properties of oligomeric silsesquioxanes stem from the well-defined nanometer sized cubic structure that can be imaged directly by AFM, as was demonstrated for various branched compounds.^{49,50} For sample preparation, 0.01 mg/mL solutions of POSS-H, PD1, and PD3 were spin-cast at 1000 rpm on a pre-cleaned silicon slide. We observed individual azo-POSS particles as well as a certain number of aggregates (Figure 6a–c) on AFM images.⁵¹ Statistical analysis revealed that the height of POSS-H particles was smaller than that of PD1 and PD3 (Figure 6d).

The sizes of POSS-H, *trans*-PD1, and *trans*-PD3 particles were estimated from 3D modeling using Chem3D. After energy minimization using the MM2 force field, the ranges of effective diameters were estimated to be 1.1–1.6, 1.4–2.7, and 1.4–3.8 nm, respectively. On the basis of AFM analysis, POSS-H height agreed well with the estimated particle diameter, and the largest fraction could be found within 0.9–1.5 nm range. The height of PD1 particles was also within the estimate of 1.2–1.8 nm, and PD3 showed a rather broad size distribution with smallest height peak of 1.2–1.5 nm. The slightly smaller height of PD3 particles could be attributed to the propensity of longer bis-azobenzene arms to adopt an extended conformation. On the other hand, for POSS-H, maxima at 2.5 and 3.3 nm could be attributed to a limited clustering of individual nanoparticles. The distribution of PD1 particles is broad, from 2.4 to 3.6 nm, and that of PD3 particles shows a maxima at 2.7 nm. Despite

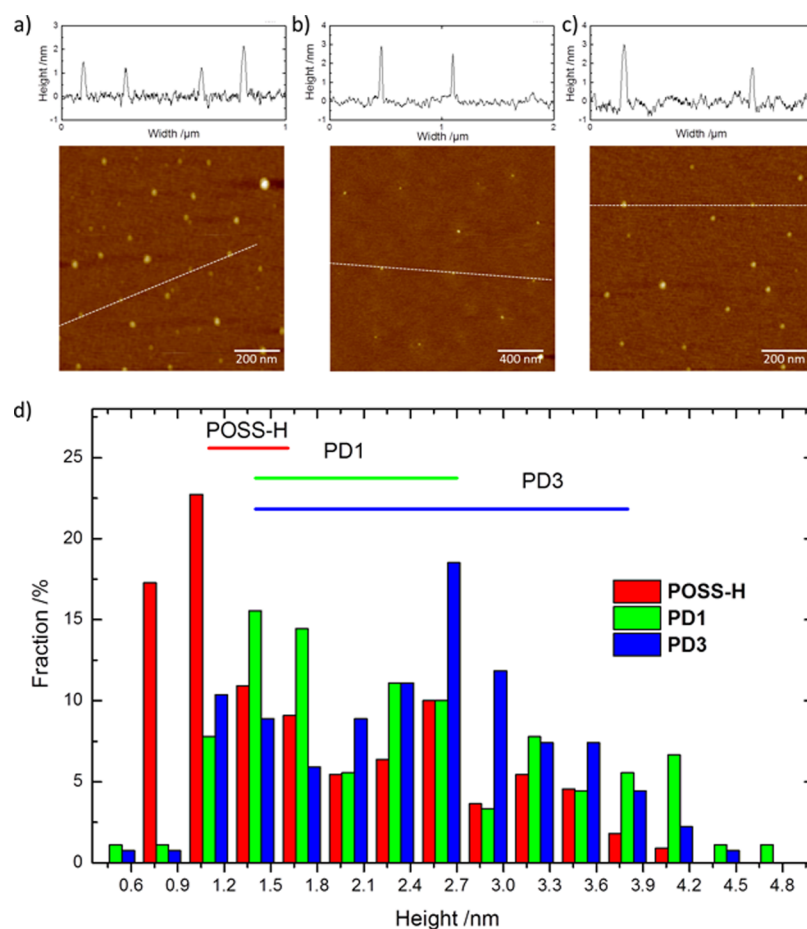


Figure 6. AFM images of (a) POSS-H, (b) PD1, and (c) PD3 individual molecules and aggregates on silicon substrates. (d) Statistical height distribution of azo-POSS particles obtained from AFM images. Horizontal lines denote the expected height ranges estimated for various molecular configurations of POSS-H and PD conjugates.

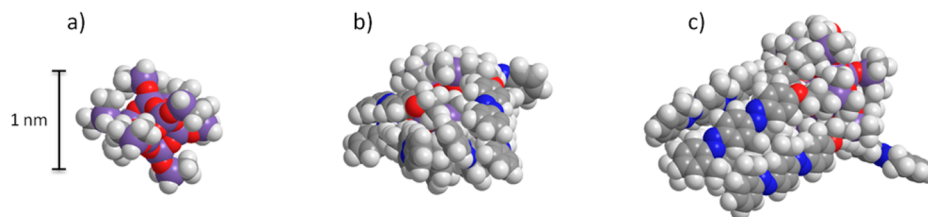


Figure 7. Molecular models of POSS derivatives: (a) POSS-H, (b) PD1, and (c) PD3.

broad distributions, the measured dimensions were in the range of dimensions estimated from molecular models for different orientations of the compounds and state of organic arms (Figure 7).

Azobenzene Isomerization in Solution and Thin Film.

Azobenzenes can undergo a rapid *trans*–*cis* photoisomerization when the π – π^* transition is excited. The back-isomerization occurs in the dark with rates dependent on the structure of azobenzene. Push–pull azobenzenes (D4) and bis-azobenzenes (D2, D3) back-isomerize instantaneously;⁵² the derivatives of 4-phenylazophenol, such as D1, however, can exist in *cis* form for many hours in the dark. Relatively slow kinetics and distinct UV–vis profiles of the *trans* and *cis* form of monoazobenzene allow monitoring the conversion with a simple spectrophotometric setup. We therefore chose D1 and PD1 as representative compounds to investigate the effect of conjugation to POSS core on the kinetics of *trans*–*cis* photoisomerization and *cis*–

trans thermal back-isomerization. Furthermore, we compared the rate constants of these processes in solution and on a thin film for the example of PD1. In order to achieve photoisomerization of azobenzene derivatives D1 and PD1, the respective 0.01 mg/mL solutions and 60 nm thin film of PD1 on quartz substrate were irradiated with 365 nm UV-light. The photoisomerization was monitored by following π – π^* absorbance at 345 nm, which corresponds to a *trans* nitrogen–nitrogen double bond. Interestingly, 4-phenylazophenol itself has a very short *cis* form lifetime and we were not able to observe the photoisomerization with conventional UV–vis spectroscopy (Supporting Information). Apparently, the etherification of phenol, even with a short allylic group, stabilizes the *cis*-azobenzene dramatically. Previously this effect was only reported for relatively long aliphatic chains.⁵³ We found that the photoisomerization reached a photostationary state within

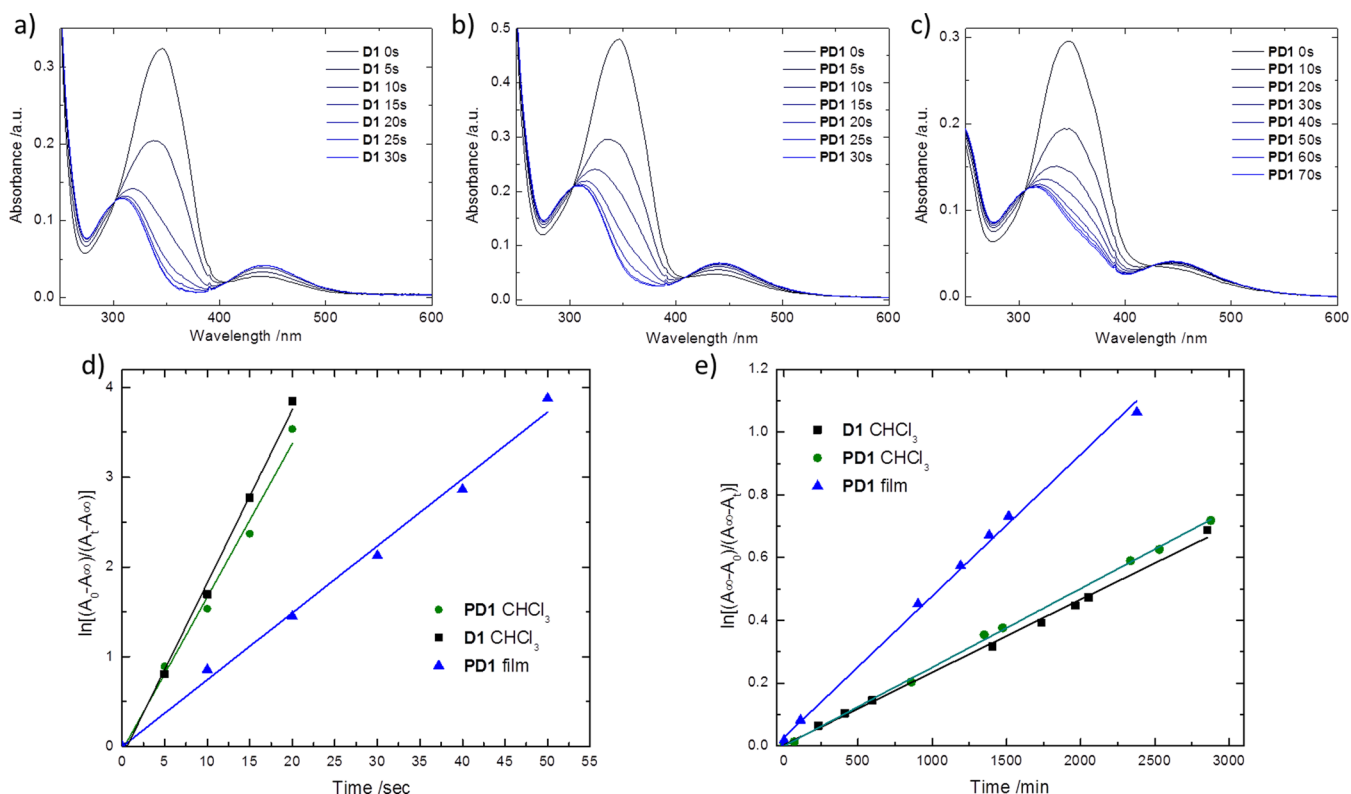


Figure 8. Photoisomerization of **D1** and **PD1**. (a) **D1** in CHCl_3 solution, (b) **PD1** in CHCl_3 solution, (c) **PD1** in a thin film. (d) Kinetics of the trans–cis photoisomerization of **D1** in CHCl_3 solution and **PD1** in CHCl_3 solution and a thin film. (e) Kinetics of cis–trans thermal isomerization of **D1** in CHCl_3 solution and **PD1** in CHCl_3 solution and a thin film.

30 s for solutions of **D1** (1.6×10^{-5} M) and **PD1** (3.6×10^{-6} M) in chloroform (Figure 8a,b).

It is worth noting that the photoisomerization of **PD1** in a thin film was slower than in solution, with a significant portion of trans isomer present even after 70 s of UV irradiation (Figure 8c). The first-order rate constant of photoisomerization can be determined from the slope of the plot of $\ln[(A_0 - A_\infty)/(A_t - A_\infty)]$ vs time,⁵⁴ where A_0 , A_∞ , and A_t are the absorbances before irradiation, after reaching a photostationary state, and at a given time, respectively.

The photoisomerization experiment was performed in triplicate for each sample, and the averaged data points along with linear fits are presented in Figure 8d. Compounds **D1** and **PD1** in chloroform solution had similar observed rate constants of 0.193 ± 0.015 and 0.186 ± 0.029 s^{-1} , respectively, which indicate that the spacer between the azobenzene and POSS core eliminates steric hindrance from grafting, which could affect the photoisomerization kinetics. Photoisomerization of **PD1** in a thin film was significantly slower, with an observed rate constant of 0.078 ± 0.010 s^{-1} , which is expected by considering the reduced free volume, which hinders the trans–cis photoisomerization through reconfiguration of a double bond.⁵⁵

Next, we studied the thermal cis–trans isomerization by monitoring the recovery of *trans*-azobenzene absorbance in irradiated samples (Figure 8e). Similarly, the rate constants can be found from the slope of a plot of $\ln[(A_\infty - A_0)/(A_\infty - A_t)]$ vs time, where A_0 , A_∞ , A_t are the absorbances after UV irradiation, after reaching a ground state, and at a given time, respectively. Again, **D1** and **PD1** relaxed to the thermodynamically more stable *trans*-azobenzene form with similar rate constants of 2.3×10^{-4} and 2.5×10^{-4} min^{-1} , respectively.

Interestingly, **PD1** in a thin film showed a higher rate constant of back-isomerization than in solution, 4.5×10^{-4} min^{-1} . This observation could be due to the high level of azobenzene aggregation, which could preferentially stabilize a more planar trans isomer; however, as mentioned previously, there was no change in azobenzene absorbance spectra of a film compared to **PD1** solution. A more likely explanation is that in solid matrix the cis isomer can be trapped in a strained conformation, which quickly relaxes back to the trans isomer.^{56,57} Furthermore, trans–cis isomerization increases the overall volume of **PD1** molecule, and the resistance of the surrounding matrix to reorganization shifts the equilibrium toward *trans*-azobenzene.⁵⁸

It is important to note that photoisomerization of **D1** and **PD1** compounds was completely reversible and can be repeated over multiple cycles (see Supporting Information). Furthermore, cis–trans back-isomerization could be achieved within several minutes by irradiating samples with white light.^{59,60} The stable trans–cis cycling could also be achieved in **PD1** ultrathin films.

In conclusion, we synthesized a series of branched azo–POSS structures based on three different azobenzenes, mono-, bis-, and push–pull azobenzenes, with suppressed crystallization and stacking ability as well as high thermal stability and nanocomposite film-forming ability. Conjugation to POSS core does not affect the kinetics of trans–cis photoisomerization and thermal cis–trans relaxation. Branched azo–POSS conjugates with preserved reversible photoisomerization and easy processability synthesized in this study can be used in photoresponsive devices for various applications as a promising photochromic medium for optical storage and sensing. These applications almost certainly will benefit from a high grafting density of

azo-POSS conjugates and hence a high photoinduced anisotropy and refractive index variation. Furthermore, the high thermal stability and low aggregation of star-shaped POSS-based conjugates may improve the performance of photo-switchable devices.

■ ASSOCIATED CONTENT

● Supporting Information

Experimental procedures, NMR and FTIR spectra of synthesized compounds, absorbance and emission spectra for D4 and PD4, AFM images of the annealed PD4 film, photoisomerization of 4-phenylazophenol, trans-cis cycling of D1 and PD1. These materials are available free of charge via the Internet at <http://pubs.acs.org>.

■ AUTHOR INFORMATION

Corresponding Author

*E-mail: vladimir@mse.gatech.edu.

Notes

The authors declare no competing financial interest.

■ ACKNOWLEDGMENTS

This work was supported by National Science Foundation, NSF-DMR grant 1002810 (synthesis of compounds and film morphology) and the Department of Energy, Office of Basic Energy Sciences, Division of Materials Sciences and Engineering under Award # DE-FG02-09ER46604 (optical properties and photoisomerization). We thank Dr. M. Chyasnachyus for the assistance with AFM measurements.

■ REFERENCES

- (1) Zhang, W. A.; Muller, A. H. E. Architecture, self-assembly and properties of well-defined hybrid polymers based on polyhedral oligomeric silsesquioxane (POSS). *Prog. Polym. Sci.* **2013**, *38*, 1121–1162.
- (2) Kuo, S. W.; Chang, F. C. POSS related polymer nanocomposites. *Prog. Polym. Sci.* **2011**, *36*, 1649–1696.
- (3) Mark, J. E. Some Interesting things about polysiloxanes. *Acc. Chem. Res.* **2004**, *37*, 946–953.
- (4) Wang, F. K.; Lu, X. H.; He, C. B. Some recent developments of polyhedral oligomeric silsesquioxane (POSS)-based polymeric materials. *J. Mater. Chem.* **2011**, *21*, 2775–2782.
- (5) Wu, J.; Mather, P. T. POSS polymers: Physical properties and biomaterials applications. *Polym. Rev.* **2009**, *49*, 25–63.
- (6) Pielichowski, K.; Njuguna, J.; Janowski, B.; Pielichowski, J. Polyhedral oligomeric silsesquioxanes (POSS)-containing nanohybrid polymers. *Adv. Polym. Sci.* **2006**, *201*, 225–296.
- (7) Li, Y. W.; Zhang, W. B.; Hsieh, I. F.; Zhang, G. L.; Cao, Y.; Li, X. P.; Wesdemiotis, C.; Lotz, B.; Xiong, H. M.; Cheng, S. Z. D. Breaking symmetry toward nonspherical janus particles based on polyhedral oligomeric silsesquioxanes: Molecular design, “click” synthesis, and hierarchical structure. *J. Am. Chem. Soc.* **2011**, *133*, 10712–10715.
- (8) Gunawidjaja, R.; Huang, F.; Gumenna, M.; Klimenko, N.; Nunnery, G. A.; Shevchenko, V.; Tannenbaum, R.; Tsukruk, V. V. Bulk and surface assembly of branched amphiphilic polyhedral oligomer silsesquioxane compounds. *Langmuir* **2009**, *25*, 1196–209.
- (9) Tanaka, K.; Chujo, Y. Advanced functional materials based on polyhedral oligomeric silsesquioxane (POSS). *J. Mater. Chem.* **2012**, *22*, 1733–1746.
- (10) Cheng, C. C.; Yen, Y. C.; Chang, F. C. Self-supporting polymer from a POSS derivative. *Macromol. Rapid Commun.* **2011**, *32*, 927–32.
- (11) Cassagneau, T.; Caruso, F. Oligosilsesquioxanes as versatile building blocks for the preparation of self-assembled thin films. *J. Am. Chem. Soc.* **2002**, *124*, 8172–8180.

- (12) Lu, C. H.; Kuo, S. W.; Huang, C. F.; Chang, F. C. Self-assembled fernlike microstructures of polyhedral oligomeric silsesquioxane/gold nanoparticle hybrids. *J. Phys. Chem. C* **2009**, *113*, 3517–3524.

- (13) Naka, K.; Fujita, M.; Tanaka, K.; Chujo, Y. Water-soluble anionic POSS-core dendrimer: Synthesis and copper(II) complexes in aqueous solution. *Langmuir* **2007**, *23*, 9057–9063.

- (14) Liras, M.; Pintado-Sierra, M.; Amat-Guerri, F.; Sastre, R. New BODIPY chromophores bound to polyhedral oligomeric silsesquioxanes (POSS) with improved thermo- and photostability. *J. Mater. Chem.* **2011**, *21*, 12803–12811.

- (15) Pu, K. Y.; Li, K.; Liu, B. Cationic oligofluorene-substituted polyhedral oligomeric silsesquioxane as light-harvesting unimolecular nanoparticle for fluorescence amplification in cellular imaging. *Adv. Mater.* **2010**, *22*, 643–646.

- (16) He, C.; Xiao, Y.; Huang, J.; Lin, T.; Mya, K. Y.; Zhang, X. Highly efficient luminescent organic clusters with quantum dot-like properties. *J. Am. Chem. Soc.* **2004**, *126*, 7792–7793.

- (17) Lo, M. Y.; Zhen, C.; Lauters, M.; Jabbour, G. E.; Sellinger, A. Organic-inorganic hybrids based on pyrene functionalized octavinyl-silsesquioxane cores for application in OLEDs. *J. Am. Chem. Soc.* **2007**, *129*, 5808–5809.

- (18) Sellinger, A.; Tamaki, R.; Laine, R. M.; Ueno, K.; Tanabe, H.; Williams, E.; Jabbour, G. E. Heck coupling of haloaromatics with octavinylsilsesquioxane: Solution processable nanocomposites for application in electroluminescent devices. *Chem. Commun.* **2005**, 3700–3702.

- (19) Merino, E. Synthesis of azobenzenes: The coloured pieces of molecular materials. *Chem. Soc. Rev.* **2011**, *40*, 3835–3853.

- (20) Beharry, A. A.; Woolley, G. A. Azobenzene photoswitches for biomolecules. *Chem. Soc. Rev.* **2011**, *40*, 4422–4437.

- (21) Sidorenko, A.; Houphouet-Boigny, C.; Villavicencio, O.; McGrath, D. V.; Tsukruk, V. V. Low generation photochromic monodendrons on a solid surface. *Thin Solid Films* **2002**, *410*, 147–158.

- (22) Sidorenko, A.; Houphouet-Boigny, C.; Villavicencio, O.; Hashemzadeh, M.; McGrath, D. V.; Tsukruk, V. V. Photoresponsive Langmuir monolayers from azobenzene-containing dendrons. *Langmuir* **2000**, *16*, 10569–10572.

- (23) Wang, D.; Wang, X. Amphiphilic azo polymers: Molecular engineering, self-assembly and photoresponsive properties. *Prog. Polym. Sci.* **2013**, *38*, 271–301.

- (24) Natansohn, A.; Rochon, P. Photoinduced motions in azo-containing polymers. *Chem. Rev.* **2002**, *102*, 4139–4175.

- (25) Wang, X. L.; Wang, X. G. Epoxy-based azo polymers with high chromophore density: Synthesis, characterization and photoinduced birefringence. *Chin. J. Polym. Sci.* **2012**, *30*, 415–422.

- (26) Kumar, S.; Koh, J. Physicochemical, circular dichroism-induced helical conformation and optical property of chitosan azo-based amino methanesulfonate complex. *J. Appl. Polym. Sci.* **2012**, *124*, 4897–4903.

- (27) Mahimwalla, Z.; Yager, K. G.; Mamiya, J.; Shishido, A.; Priimagi, A.; Barrett, C. J. Azobenzene photomechanics: Prospects and potential applications. *Polym. Bull.* **2012**, *69*, 967–1006.

- (28) Barrett, C. J.; Mamiya, J. I.; Yager, K. G.; Ikeda, T. Photo-mechanical effects in azobenzene-containing soft materials. *Soft Matter* **2007**, *3*, 1249–1261.

- (29) Brzozowski, L.; Sargent, E. H. Azobenzenes for photonic network applications: Third-order nonlinear optical properties. *J. Mater. Sci.: Mater. Electron.* **2001**, *12*, 483–489.

- (30) Emoto, A.; Uchida, E.; Fukuda, T. Optical and physical applications of photocontrollable materials: Azobenzene-containing and liquid crystalline polymers. *Polymers* **2012**, *4*, 150–186.

- (31) Chi, H.; Mya, K. Y.; Lin, T. T.; He, C. B.; Wang, F. K.; Chin, W. S. Thermally stable azobenzene dyes through hybridization with POSS. *New J. Chem.* **2013**, *37*, 735–742.

- (32) Zhou, J. L.; Zhao, Y. C.; Yu, K. C.; Zhou, X. P.; Xie, X. L. Synthesis, thermal stability and photoresponsive behaviors of azobenzene-tethered polyhedral oligomeric silsesquioxanes. *New J. Chem.* **2011**, *35*, 2781–2792.

- (33) Miniewicz, A.; Girones, J.; Karpinski, P.; Mossety-Leszczak, B.; Galina, H.; Dutkiewicz, M. Photochromic and nonlinear optical properties of azo-functionalized POSS nanoparticles dispersed in nematic liquid crystals. *J. Mater. Chem. C* **2014**, *2*, 432–440.
- (34) Meng, X.; Natansohn, A.; Rochon, P. Azo polymers for reversible optical storage. 13. Photoorientation of rigid side groups containing two azo bonds. *Polymer* **1997**, *38*, 2677–2682.
- (35) Feher, F. J.; Wyndham, K. D.; Soulivong, D.; Nguyen, F. Syntheses of highly functionalized cube–octameric polyhedral oligosilsesquioxanes (R₈Si₈O₁₂). *J. Chem. Soc., Dalton Trans.* **1999**, 1491–1497.
- (36) Cordes, D. B.; Lickiss, P. D.; Rataboul, F. Recent developments in the chemistry of cubic polyhedral oligosilsesquioxanes. *Chem. Rev.* **2010**, *110*, 2081–173.
- (37) Lickiss, P. D.; Rataboul, F. Fully condensed polyhedral oligosilsesquioxanes (POSS): From synthesis to application. In *Advances in Organometallic Chemistry*; Hill, A. F., Fink, M. J., Eds.; Elsevier Academic Press Inc: San Diego, CA, 2008; Vol. 57, pp 1–116.
- (38) Marciniak, B.; Maciejewski, H.; Pietraszuk, C.; Pawluc, P. *Hydrosilylation: A Comprehensive Review on Recent Advances*; Marciniak, B., Ed.; Springer: Berlin, 2009; p 7.
- (39) Kawai, T.; Umemura, J.; Takenaka, T. UV absorption-spectra of azobenzene-containing long-chain fatty-acids and their barium salts in spread monolayers and Langmuir–Blodgett films. *Langmuir* **1989**, *5*, 1378–1383.
- (40) Toro, C.; Thibert, A.; De Boni, L.; Masunov, A. E.; Hernandez, F. E. Fluorescence emission of disperse red 1 in solution at room temperature. *J. Phys. Chem. B* **2008**, *112*, 929–937.
- (41) Han, M. N.; Norikane, Y.; Onda, K.; Matsuzawa, Y.; Yoshida, M.; Hara, M. Light-driven modulation of fluorescence color from azobenzene derivatives containing electron-donating and electron-withdrawing groups. *New J. Chem.* **2010**, *34*, 2892–2896.
- (42) Zayed, M. A.; Mohamed, G. G.; Fahmey, M. A. Thermal and mass spectral characterization of novel azo dyes of *p*-acetoamidophenol in comparison with Hammett substituent effects and molecular orbital calculations. *J. Therm. Anal. Calorim.* **2012**, *107*, 763–776.
- (43) Blanco, I.; Abate, L.; Bottino, F. A.; Bottino, P.; Chiacchio, M. A. Thermal degradation of differently substituted cyclopentyl polyhedral oligomeric silsesquioxane (CP-POSS) nanoparticles. *J. Therm. Anal. Calorim.* **2012**, *107*, 1083–1091.
- (44) Mantz, R. A.; Jones, P. F.; Chaffee, K. P.; Lichtenhan, J. D.; Gilman, J. W.; Ismail, I. M. K.; Burmeister, M. J. Thermolysis of polyhedral oligomeric silsesquioxane (POSS) macromers and POSS–siloxane copolymers. *Chem. Mater.* **1996**, *8*, 1250–1259.
- (45) Fina, A.; Tabuani, D.; Carniato, F.; Frache, A.; Boccaleri, E.; Camino, G. Polyhedral oligomeric silsesquioxanes (POSS) thermal degradation. *Thermochim. Acta* **2006**, *440*, 36–42.
- (46) Cheng, C. C.; Chien, C. H.; Yen, Y. C.; Ye, Y. S.; Ko, F. H.; Lin, C. H.; Chang, F. C. A new organic/inorganic electroluminescent material with a silsesquioxane core. *Acta Mater.* **2009**, *57*, 1938–1946.
- (47) Sastre, R.; Martin, V.; Garrido, L.; Chiara, J. L.; Trastoy, B.; Garcia, O.; Costela, A.; Garcia-Moreno, I. Dye-doped polyhedral oligomeric silsesquioxane (POSS)-modified polymeric matrices for highly efficient and photostable solid-state lasers. *Adv. Funct. Mater.* **2009**, *19*, 3307–3316.
- (48) Shevchenko, V. V.; Sidorenko, A. V.; Bliznyuk, V. N.; Tkachenko, I. M.; Shekera, V.; Smirnov, N. N.; Maslyanitsyn, I. A.; Shigorin, V. D.; Yakimansky, A. V.; Tsukruk, V. V. Synthesis and properties of hydroxylated core-fluorinated diamines and polyurethanes based on them with azobenzene nonlinear optical chromophores in the backbone. *Polymer* **2013**, *54*, 6516–6525.
- (49) Sidorenko, A.; Zhai, X. W.; Peleshanko, S.; Greco, A.; Shevchenko, V. V.; Tsukruk, V. V. Hyperbranched polyesters on solid surfaces. *Langmuir* **2001**, *17*, 5924–5931.
- (50) McConney, M. E.; Singamaneni, S.; Tsukruk, V. V. Probing soft matter with the atomic force microscopies: Imaging and force spectroscopy. *Polymer Rev.* **2010**, *50*, 235–286.
- (51) Mori, H.; Yamada, M. Synthesis and characterization of cationic silsesquioxane hybrids by hydrolytic condensation of triethoxysilane derived from 2-(dimethylamino)ethyl acrylate. *Colloid Polym. Sci.* **2012**, *290*, 1879–1891.
- (52) Sheng, C.; Norwood, R. A.; Wang, J.; Thomas, J.; Wu, Y.; Zheng, Z.; Tabirian, N.; Steeves, D. M.; Kimball, B. R.; Peyghambarian, N. Time-resolved studies of photoinduced birefringence in azobenzene dye-doped polymer films. *Appl. Opt.* **2008**, *47*, 5074–5077.
- (53) Han, M. R.; Hara, M. Chain length-dependent photoinduced formation of azobenzene aggregates. *New J. Chem.* **2006**, *30*, 223–227.
- (54) Sasaki, T.; Ikeda, T.; Ichimura, K. Photoisomerization and thermal-isomerization behavior of azobenzene derivatives in liquid-crystalline polymer matrices. *Macromolecules* **1993**, *26*, 151–154.
- (55) Sin, S. L.; Gan, L. H.; Hu, X.; Tam, K. C.; Gan, Y. Y. Photochemical and thermal isomerizations of azobenzene-containing amphiphilic diblock copolymers in aqueous micellar aggregates and in film. *Macromolecules* **2005**, *38*, 3943–3948.
- (56) Imai, Y.; Naka, K.; Chujo, Y. Isomerization behavior of azobenzene chromophores attached to the side chain of organic polymer in organic–inorganic polymer hybrids. *Macromolecules* **1999**, *32*, 1013–1017.
- (57) Wu, A. P.; Talham, D. R. Photoisomerization of azobenzene chromophores in organic/inorganic zirconium phosphonate thin films prepared using a combined Langmuir–Blodgett and self-assembled monolayer deposition. *Langmuir* **2000**, *16*, 7449–7456.
- (58) Matsumoto, M.; Miyazaki, D.; Tanaka, M.; Azumi, R.; Manda, E.; Kondo, Y.; Yoshino, N.; Tachibana, H. Reversible light-induced morphological change in Langmuir–Blodgett films. *J. Am. Chem. Soc.* **1998**, *120*, 1479–1484.
- (59) Lin, Y.; Zhang, Y.; Qiao, Y.; Huang, J.; Xu, B. Light and host-guest inclusion mediated salmon sperm DNA/surfactant interactions. *J. Colloid Interface Sci.* **2011**, *362*, 430–438.
- (60) Shang, T. G.; Smith, K. A.; Hatton, T. A. Photoresponsive surfactants exhibiting unusually large, reversible surface tension changes under varying illumination conditions. *Langmuir* **2003**, *19*, 10764–10773.